



DEVCOM DAC-TN-2022-014  
July 2022

# A Methodology for Measuring Atmospheric Downwelling Path Radiance

by Bryan L. Holtsberry

### **DISCLAIMER**

The findings in this report are not to be construed as an official Department of the Army position unless so specified by other official documentation.

### **WARNING**

Information and data contained in this document are based on the input available at the time of preparation.

### **TRADE NAMES**

The use of trade names in this report does not constitute an official endorsement or approval of the use of such commercial hardware or software. The report may not be cited for purposes of advertisement.



DEVCOM DAC-TN-2022-014  
July 2022

---

# A Methodology for Measuring Atmospheric Downwelling Path Radiance

by Bryan L. Holtsberry  
*DEVCOM Analysis Center*

<b>REPORT DOCUMENTATION PAGE</b>			<i>Form Approved</i> <i>OMB No. 0704-0188</i>		
Public reporting burden for this collection of information is estimated to average 1 hour per response, including the time for reviewing instructions, searching existing data sources, gathering and maintaining the data needed, and completing and reviewing this collection of information. Send comments regarding this burden estimate or any other aspect of this collection of information, including suggestions for reducing this burden to Department of Defense, Washington Headquarters Services, Directorate for Information Operations and Reports (0704-0188), 1215 Jefferson Davis Highway, Suite 1204, Arlington, VA 22202-4302. Respondents should be aware that notwithstanding any other provision of law, no person shall be subject to any penalty for failing to comply with a collection of information if it does not display a currently valid OMB control number. <b>PLEASE DO NOT RETURN YOUR FORM TO THE ABOVE ADDRESS.</b>					
<b>1. REPORT DATE</b> July 2022		<b>2. REPORT TYPE</b> Technical Note		<b>3. DATES COVERED (From - To)</b> September 2021–June 2022	
<b>4. TITLE AND SUBTITLE</b> A Methodology for Measuring Atmospheric Downwelling Path Radiance			<b>5a. CONTRACT NUMBER</b>		
			<b>5b. GRANT NUMBER</b>		
			<b>5c. PROGRAM ELEMENT NUMBER</b>		
<b>6. AUTHOR(S)</b> Bryan L. Holtsberry			<b>5d. PROJECT NUMBER</b>		
			<b>5e. TASK NUMBER</b>		
			<b>5f. WORK UNIT NUMBER</b>		
<b>7. PERFORMING ORGANIZATION NAME(S) AND ADDRESS(ES)</b> Director DEVCOM Analysis Center White Sands Missile Range, NM 88002			<b>8. PERFORMING ORGANIZATION REPORT NUMBER</b>  DEVCOM DAC-TN-2022-014		
<b>9. SPONSORING / MONITORING AGENCY NAME(S) AND ADDRESS(ES)</b>			<b>10. SPONSOR/MONITOR'S ACRONYM(S)</b>		
			<b>11. SPONSOR/MONITOR'S REPORT NUMBER(S)</b>		
<b>12. DISTRIBUTION / AVAILABILITY STATEMENT</b> DISTRIBUTION STATEMENT A. Approved for public release: distribution unlimited.					
<b>13. SUPPLEMENTARY NOTES</b>					
<b>14. ABSTRACT</b> This report describes a methodology for measuring atmospheric downwelling path radiance (DPR). The DPR is a combination of solar scattering and emission and absorption from aerosols and gaseous molecules in the atmosphere. These processes that create DPR are briefly described, as is the instrument used to measure DPR. Measured infrared spectral DPR data are presented and compared to modeled DPR data. The measured and modeled DPR data are shown to be in good agreement, which provides confidence in the validity of the measured DPR data.					
<b>15. SUBJECT TERMS</b> infrared, downwelling path radiance, FTIR spectrometer, emission, absorption, scattering, MODTRAN					
<b>16. SECURITY CLASSIFICATION OF:</b>			<b>17. LIMITATION OF ABSTRACT</b>  UU	<b>18. NUMBER OF PAGES</b>  20	<b>19a. NAME OF RESPONSIBLE PERSON</b> Bryan L. Holtsberry
<b>a. REPORT</b> UNCLASSIFIED	<b>b. ABSTRACT</b> UNCLASSIFIED	<b>c. THIS PAGE</b> UNCLASSIFIED			<b>19b. TELEPHONE NUMBER</b> (include area code) (575) 678-4225

---

---

## Table of Contents

List of Figures .....	iv
1. INTRODUCTION .....	1
2. ATMOSPHERIC PROCESSES .....	2
3. EXPERIMENTAL METHODS .....	4
4. INSTRUMENTATION .....	5
5. RESULTS AND DISCUSSION .....	9
6. CONCLUSION.....	11
7. REFERENCES .....	12
List of Acronyms .....	13
Distribution List .....	14

---

---

## List of Figures

Figure 1.	Atmospheric path radiance in the MWIR spectral region .....	3
Figure 2.	Atmospheric transmission in the MWIR spectral region.....	3
Figure 3.	Experimental setup for DPR measurement.....	4
Figure 4.	Michelson interferometer configuration .....	5
Figure 5.	Sample interferogram created by an FTIR.....	7
Figure 6.	Bomem MR304 FTS with 5-mrad telescope attached .....	8
Figure 7.	Downwelling radiance data measured with the Bomem on 9 April 2022 at 2132 local time.....	9
Figure 8.	Downwelling radiance data on 9 April 2022 at 2132 local time, modeled with MODTRAN .....	10

---

---

# 1. INTRODUCTION

This technical note (TN) describes a methodology used by the U.S. Army Combat Capabilities Development Command (DEVCOM) Analysis Center for spectral measurement of downwelling path radiance (DPR). DPR is the radiance from the sky that is incident on the ground and includes contributions from aerosol scattering, as well as emission and absorption from atmospheric gases. A Fourier transform infrared (FTIR) spectrometer is used to measure DPR, and the result is calibrated spectral radiance in the mid-wave infrared (MWIR) and long-wave infrared (LWIR) spectral regions. Measured DPR data can be used to estimate atmospheric parameters such as ambient temperature, relative humidity, cloud cover, transmission, and more.

In this TN, we provide a short description of the theory and physical mechanisms that contribute to the DPR, offer details on FTIR spectrometer systems, and conclude with samples of measured spectral DPR data. Subsequent sections will provide a description of the experimental setup used during the DPR measurement and FTIR spectrometer theory. We will show the measured DPR and provide a brief analysis of the data.

---

---

## 2. ATMOSPHERIC PROCESSES

A brief description of the atmospheric mechanisms responsible for the DPR is given here. It is important to note that we are not atmospheric scientists, and a rigorous description is beyond the scope of this TN.

The atmosphere surrounds the Earth and protects it from harmful radiation, such as ultraviolet (UV) radiation, and objects such as meteors. The atmosphere comprises gases and aerosols (suspended particles) at temperatures and pressures that vary with altitude.<sup>1</sup> Most of the gases and aerosols are found in the troposphere, which is a layer of the atmosphere that extends from the ground to an altitude of about 11 km.<sup>1</sup>

The total sky radiance incident on the Earth's surface includes components from scattered solar radiation and emission from gases in the atmosphere. The scattered radiation only occurs when the sun is out and is more pronounced at shorter wavelengths, such as the visible (VIS) and near-infrared (NIR).<sup>2</sup> The gaseous emission is present during all hours and is more pronounced at longer wavelengths, such as the LWIR.<sup>3</sup>

In 1859, Gustav Kirchoff developed his laws of spectroscopy.<sup>4</sup> These laws describe the spectra emitted by an object, depending on its temperature, state, and pressure. There are three laws, and they can be stated as follows:

1. A hot solid or liquid, or a gas under high pressure, will emit a continuous spectrum (also known as a continuum).
2. A hot gas, when under low pressure, will emit discrete narrow emission lines.
3. When a hot gas under low pressure is in front of an object that is emitting a continuum, the gas will absorb a portion of the emitted continuum, resulting in an absorption spectrum. The wavelength of the absorption features is the same as the emission lines for the gas.

The atmospheric radiance created from solar scattering and thermal emission is called the path radiance.<sup>5</sup> This path radiance is absorbed by atmospheric gases such as water (H<sub>2</sub>O) and carbon dioxide (CO<sub>2</sub>) that are between the sensor and target. Plots of path radiance and atmospheric absorption in the MWIR spectral region are shown in Figures 1 and 2, respectively. The plots were created using the MODerate resolution atmospheric TRANsmiission (MODTRAN) atmospheric modeling software.<sup>6</sup>

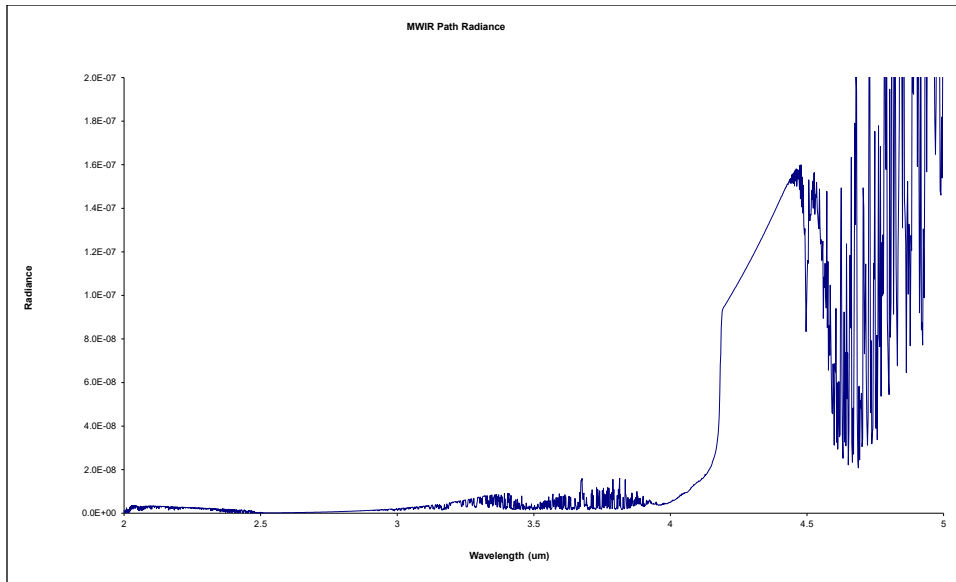


**Figure 1. Atmospheric path radiance in the MWIR spectral region**

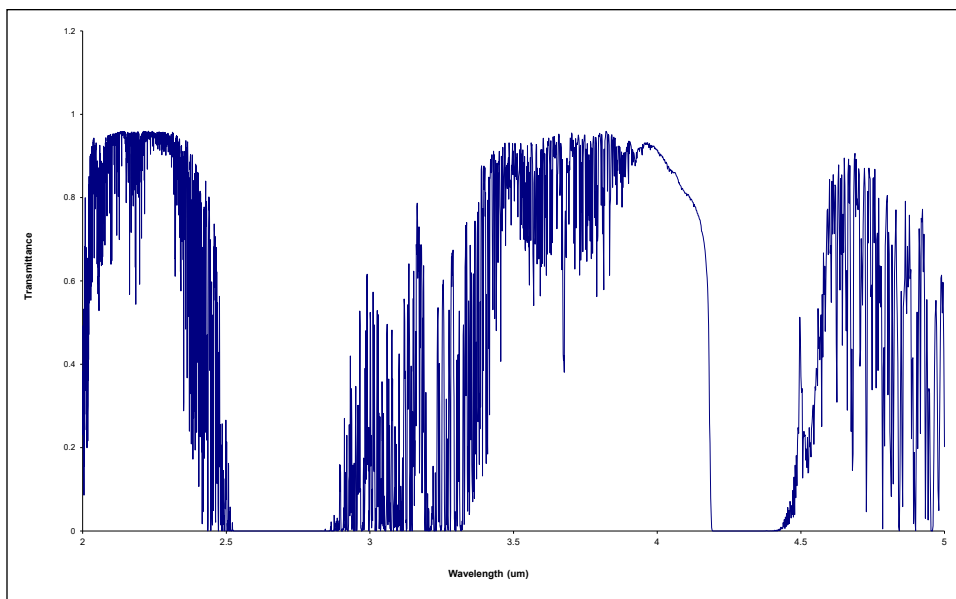


**Figure 2. Atmospheric transmission in the MWIR spectral region**

---

---

### 3. EXPERIMENTAL METHODS

The experimental setup for DPR measurement is depicted in Figure 3. A plane mirror was mounted on a tripod and tilted at an angle of 45°. The tilted mirror was placed directly in front of the FTIR spectrometer, which is also mounted on a tripod. This configuration ensures that the spectrometer's field of view (FOV) is filled with the DPR. Immediately after data of the DPR are collected, the FTIR is calibrated by measuring large area blackbody (LABB) calibration sources that are operated at two different temperatures. One of the LABBs is set at a temperature less than the ambient air temperature, and the other is set at a temperature greater than the ambient air temperature. The spectral exitance of the LABB at a given temperature is calculated from Planck's law, as given by Equation (1).<sup>7</sup>

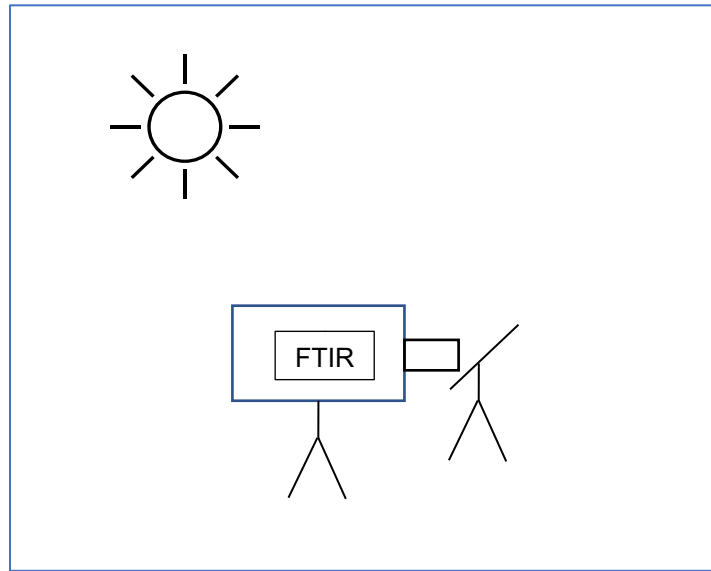


Figure 3. Experimental setup for DPR measurement

$$L_{\lambda}(\lambda, T) = \frac{2hc^2}{\lambda^5 \left( e^{\left\{ \frac{hc}{\lambda kT} \right\}} - 1 \right)} \quad (1)$$

where  $T$  is the blackbody temperature (K),

$\lambda$  (m) is the wavelength,

$h = 6.626 \times 10^{-34}$  (J\*s) is the Planck constant,

$c = 2.998 \times 10^8$  (m/s) is the speed of light, and

$k = 1.381 \times 10^{-23}$  (J/K) is the Boltzmann constant.

---

---

## 4. INSTRUMENTATION

This section provides a theoretical description of the FTIR spectrometer used to measure the DPR. We start by describing the Michelson interferometer, which is the basis for the FTIR, and then describe the specific FTIR used by the DEVCOM Analysis Center (DAC) for the DPR measurements. Much of this material comes from the author's New Mexico State University master's thesis.<sup>8</sup>

At the heart of an FTIR is something called a Michelson interferometer, which was invented by Albert A. Michelson in 1880.<sup>9</sup> The Michelson interferometer consists of two flat mirrors located at 90° to each other with a beam splitter mounted on the 45° line that separates the two mirrors (Figure 4). A beam of radiation from a source is divided into two distinct paths at the beam splitter. One of the reflecting mirrors is typically mounted on a movable micrometer, which allows the path length of the corresponding beam to be changed, thus changing the phase relationship between the two beams. When the two beams recombine, they interfere with each other, which creates a “fringe” irradiance pattern at the detector.

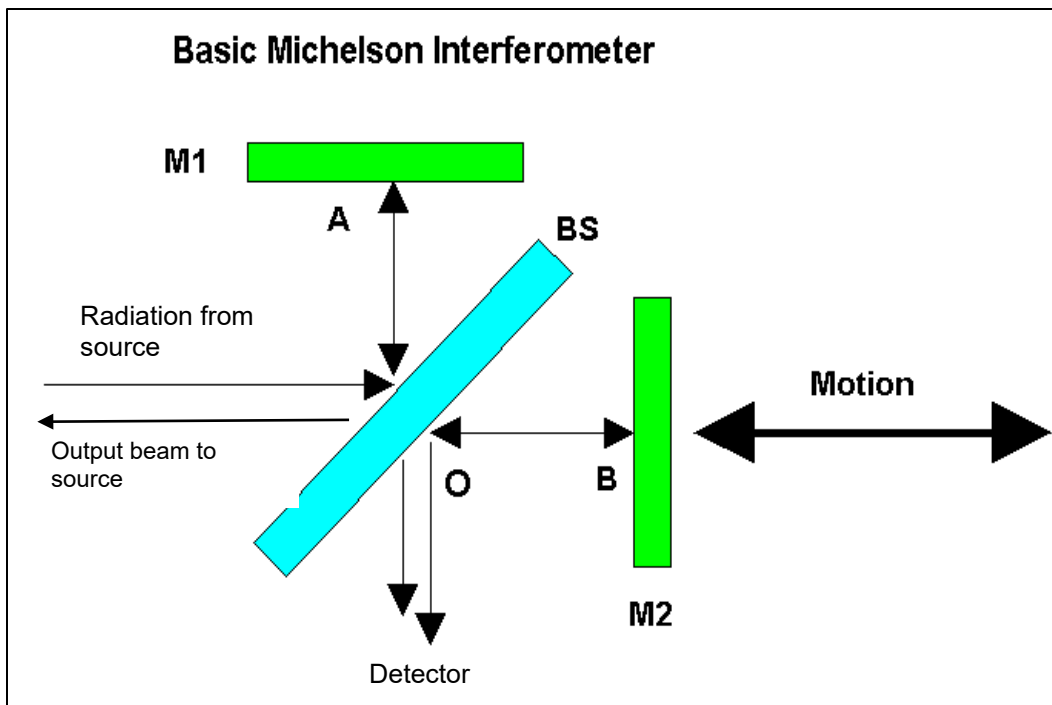


Figure 4. Michelson interferometer configuration

---

---

The difference in path length between the two beams is called optical path difference (OPD) or retardation and is normally denoted by the Greek letter  $\delta$ . As indicated in Figure 4, after the beams that are split from the input beam reflect off the mirrors and recombine at the beam splitter, two output beams are created. One of the output beams is reflected to the detector and the other beam is transmitted out of the front of the interferometer in the direction of the light source.

Strictly speaking, the movable mirror in a Michelson interferometer is not moved in a continuous fashion. An FTIR is a variant of the Michelson interferometer, in which the movable mirror is moved rapidly at a constant velocity. When the mirror has traveled the required distance, which is dictated by the required spectral resolution, it is quickly returned to the start position to begin the next scan.

During the motion of the moving mirror, each wavelength of the light from the source is modulated at a unique frequency that is a function of the wavelength of the light and the velocity of the moving mirror. As the mirror is moved, the two beams interfere with different phases. This creates irradiance variations due to interference. At a given retardation, the interference is constructive for some frequencies and destructive for others. Because the retardation is constantly changing, the various frequencies present in the beam are modulated at different rates.

The interference pattern created from the two modulated beams is called an interferogram, since it results from the interference of all the wavelengths contained in the input beam.<sup>9</sup> An interferogram is the electrical signal at the output of the detector as a function of the retardation and is a coded representation of the target spectrum. A plot of an interferogram is shown in Figure 5. The peak amplitude near the center of the interferogram is known as the zero-path difference (ZPD) point. This is the point in the scan where the mirrors are equidistant from the beam splitter and  $\delta=0$ .

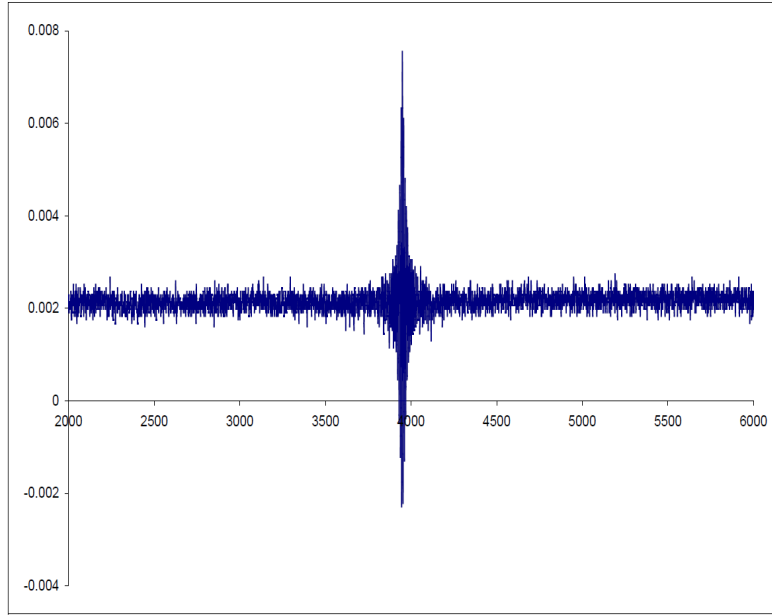


**Figure 5. Sample interferogram created by an FTIR**

For monochromatic light of intensity  $I_o$ , the intensity of the interferogram as a function of retardation ( $\delta = 2(OB - OA)$  in Figure 4) and wavenumber ( $\nu = 1/\lambda$ ) is given by

$$I(\delta, \nu) = (I_o / 2)[1 + \cos(2\pi\nu\delta)] \quad (2)$$

For polychromatic light, the total intensity of the interferogram is the sum of the monochromatic interferograms as given by

$$I(\delta) = \int I(\delta, \nu) d\nu = \int (I_o / 2)[1 + \cos(2\pi\nu\delta)] d\nu \quad (3)$$

The interferogram is just a Fourier cosine transform of the incoming light from the source. Therefore, by computing the inverse Fourier transform of the interferogram, we obtain the spectral radiance of the source.<sup>9</sup>

The DPR data presented in this TN were collected using a Bomem model MR304 FTIR. It is a two-detector system that is spectrally responsive from 2 to 15  $\mu\text{m}$ . Indium antimonide (InSb) and mercury cadmium telluride (MCT) detectors are used, where both are cooled with Stirling coolers. The spectral resolution and scan rate are inversely proportional to each other and are selected for a particular experiment based on the data requirements for that experiment. As the spectral resolution is increased (smaller wavenumber value), the length of each scan is also increased, and this results in a lower scan rate. The spectral resolution varies from 1 wavenumber ( $\text{cm}^{-1}$ ) to 128  $\text{cm}^{-1}$ . The scan rate varies from 7 scans per second at 1  $\text{cm}^{-1}$  and 130 scans per second at

---

---

128  $\text{cm}^{-1}$ . There are three telescopes available for the FTIR with FOVs of 5 mrad, 28 mrad, and 75 mrad. The MR304 spectrometer with the 5-mrad telescope attached is shown in Figure 6.

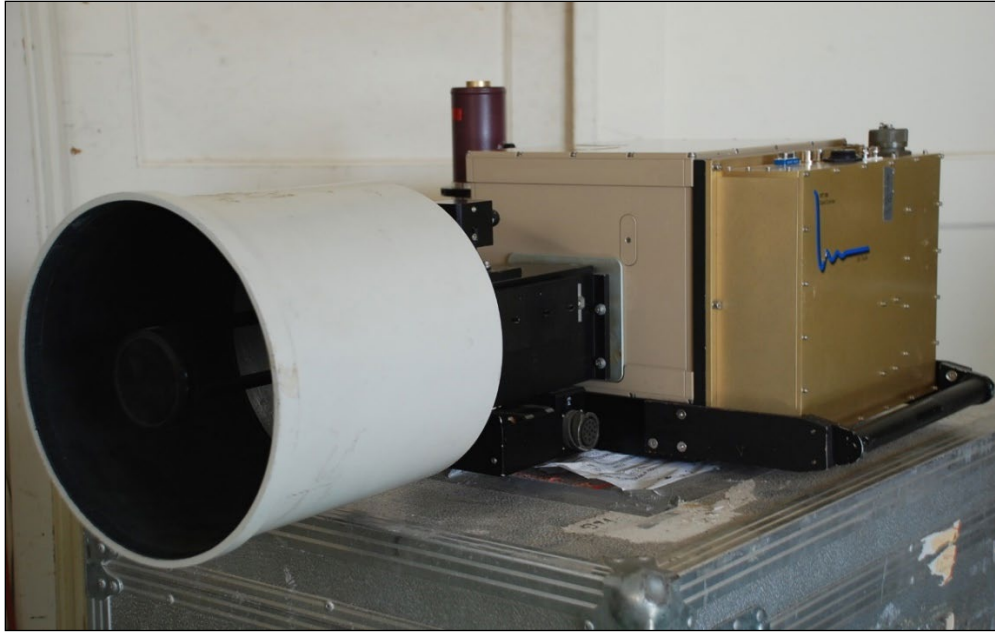


**Figure 6. Bomem MR304 FTS with 5-mrad telescope attached**

The Bomem FTIR utilizes the “wishbone arm” modulator consisting of an arm that pivots on an axis and retroreflectors, which was developed by Bomem. A diagram of the interferometer system is shown in Figure 7. Unlike traditional Michelson interferometers, no light is reflected out of the input telescope, so it has much better sensitivity. This is done using parabolic mirrors that reflect the two beams up at an angle of  $30^\circ$  from the optical axis into the upper part of the interferometer.

The second input beam is from an  $\text{LN}_2$  dewar attached to the side of the FTIR and is seen in Figure 6 (the burgundy dewar). Operating the Bomem with the dewar attached to the second input port compensates for the internal emissions of the FTIR. The emissions add noise to the measured signal.

The Bomem FTIR incorporates a HeNe laser and “white light source” in the interferometer. Light from both these sources is modulated and detected to synchronize the digitization of the interferogram at the ZPD point. Digitization of the interferogram requires precise monitoring of the OPD in the interferometer. The monochromatic laser radiation gives a sinusoidal interferogram that is detected and digitized to provide the OPD information. Digitization of the IR interferogram is triggered at the zero crossings of the laser fringe signal. The laser signal is also used to derive wavenumber information.

---

---

## 5. RESULTS AND DISCUSSION

Samples of measured and modeled DPR data are presented in this section. The measured data were collected on 9 April 2022 at 2132 local time at a tropical location. The ambient air temperature at the time of the measurement was about 75 °F and the dew point was 65 °F, as reported by a local weather website. The raw data were calibrated with measurements of LABBs operated at temperatures of 23 °C and 150 °C. Plots of calibrated DPR data are shown in Figure 7. Both figures show the radiance calculated for a blackbody at 75 °F (from Equation (1)) and the measured spectral radiance. In accordance with Kirchoff's first law of spectroscopy, the DPR was modeled as a continuum and calculated using Planck's law. There is a plethora of more sophisticated models to calculate atmospheric effects,<sup>10,11</sup> but we chose to use Planck's law for this comparison. Data collected with the InSb detector is shown in the left plot, and data collected with the MCT detector in the right plot.

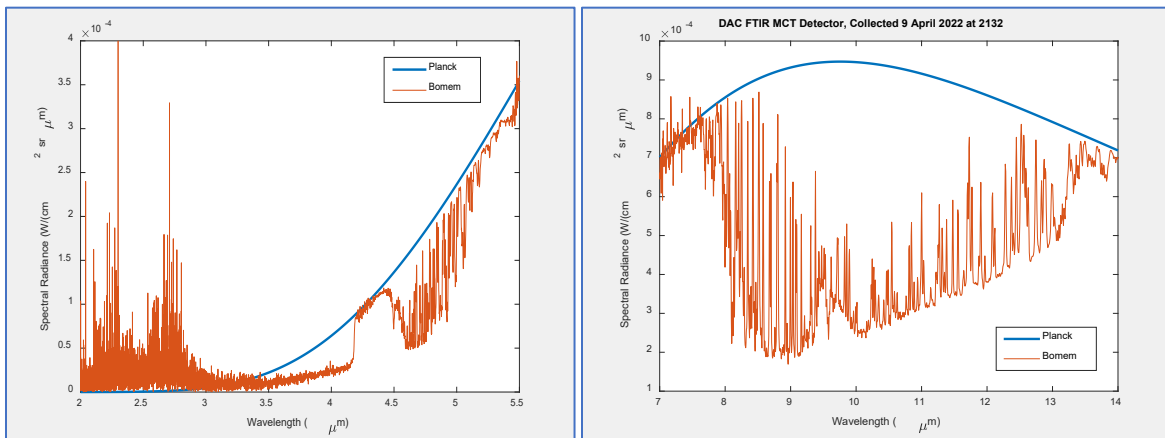


**Figure 7. Downwelling radiance data measured with the Bomem on 9 April 2022 at 2132 local time**

As a sanity check, the DPR was modeled with MODTRAN and the results are shown in Figure 8. The model was run for the same date and time as the measured data. The modeled spectral radiance is in good agreement with the measured spectral radiance, in terms of both the curve shapes and amplitudes, although there are some differences. In particular, the emissions seen from about 2 to 3 μm in the measured data are not as pronounced in the modeled data. Also, the modeled data are less noisy at the upper end of the MWIR plot and the lower end of the LWIR plot. It is a fairly common practice to run dry gaseous nitrogen into an FTIR to purge H<sub>2</sub>O and CO<sub>2</sub> from the instrument's interior. We do not have this capability for our FTIR and this may have noise in the data.

The molecules that absorb or emit radiation in a particular spectral region are identified in the plots. The primary absorbing molecules in the MWIR and LWIR spectral regions are H<sub>2</sub>O and CO<sub>2</sub>.<sup>1</sup> Absorption consists of both local-line and continuum absorption.<sup>1</sup>

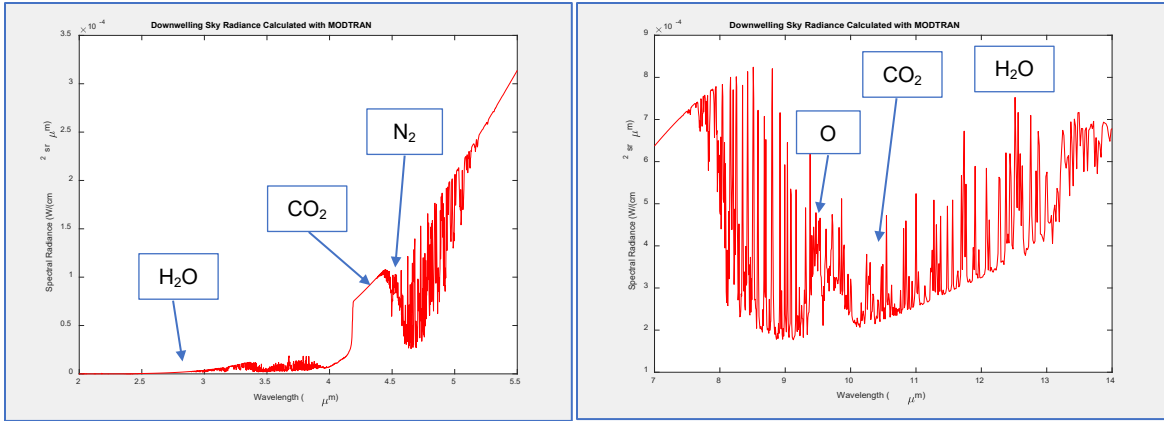


Figure 8. Downwelling radiance data on 9 April 2022 at 2132 local time, modeled with MODTRAN

---

---

## 6. CONCLUSION

In this TN we described a process for measuring the DPR. The atmospheric mechanisms that create the DPR were discussed, as was the FTIR spectrometer used to measure DPR. We presented measured spectral DPR data and compared it to modeled DPR spectra that were created using the MODTRAN atmospheric modeling software. The measured and modeled data were in good agreement in terms of both the curve shapes and amplitudes. The measured data contained some features not seen in the modeled data. It is possible that the extra features were caused by H<sub>2</sub>O and CO<sub>2</sub> inside the FTIR. It is common practice to run dry gaseous nitrogen into an FTIR to purge these gases, but our Bomem FTIR lacks this capability.

The measured data were compared to the theoretical radiance of the sky, calculated from Planck's law for an object at the ambient air temperature at the time of the measurement. The measurement was done during nighttime hours, therefore there were no solar scattering effects in the measured DPR data. We identified specific atmospheric molecules that absorb and emit in the plots created from MODTRAN. We discussed Kirchoff's three laws of spectroscopy and saw how the DPR can be described by these laws. Specifically, molecules in the atmosphere are heated by the sun and emit a continuum. The continuum is absorbed by cooler molecules in the path between the emission and the ground, and this absorption is a combination of local-line and continuum absorption. The good agreement between measured and modeled DPR data provides confidence in our measurements and the methodology utilized for the measurements.

---

---

## 7. REFERENCES

1. Smith, F. G. (Ed.). (1993). *The infrared and electro-optical systems handbook, vol. 2, atmospheric propagation of radiation*. Copublished by the Environmental Research Institute of Michigan and SPIE Optical Engineering Press.
2. Bohren, C. F. (n.d.). *Atmospheric optics*. Pennsylvania State University, Department of Meteorology.
3. Goforth, M. A., Gilchrist, G. W., & Sirianni, J. D. (2002, March 15). Cloud effects on thermal downwelling sky radiance. *Proc. SPIE 4710, Thermosense XXIV*. doi: 10.1117/12.459570.
4. Kirchhoff's laws. (2022, June 2). *A dictionary of astronomy* (3<sup>rd</sup> ed.). Oxford University Press.  
<https://www.oxfordreference.com/view/10.1093/acref/9780191851193.001.0001/acref-9780191851193-e-2021>.
5. Hodgkin, V. A., Maurer, T., Halford, C., & Vollmerhausen, R. (2007, May 2). Impact of path radiance on MWIR and LWIR imaging. *Proc. SPIE 6543, Infrared Imaging Systems: Design, Analysis, Modeling, and Testing XVIII, 65430O*. doi: 10.1117/12.721364.
6. Berk, A., van den Bosch, J., Hawes, F., Perkins, T., Conforti, P. F., Acharya, P. K., Anderson, G. P., & Kennett, R. G. (2019, September). *MODTRAN 6.0 user's manual* (SSI-TR-685). Spectral Sciences, Inc.
7. Dereniak, E. L. & Boreman, G. D. (1996). *Infrared detectors and systems*. John Wiley & Sons, Inc.
8. Holtsberry, B. L. (2009, November 18). *A study of spectroscopic data collection and analysis techniques* [Master's thesis, New Mexico State University].
9. Bell, R. J. (1972). *Introductory Fourier transform spectroscopy*. Academic Press Inc.
10. O'Brien, S. G. & Shirkey, R. C. (2004, September). *Determination of atmospheric path radiance: Sky-to-ground ratio for wargamers* (ARL-TR-3285). U.S. Army Research Laboratory.
11. Wurst, N. P. (2017, May). *Improved atmospheric characterization for hyperspectral exploitation*. [Master's thesis, Air Force Institute of Technology].

---

---

## LIST OF ACRONYMS

CO <sub>2</sub>	carbon dioxide
DAC	DEVCOM Analysis Center
DEVCOM	U.S. Army Combat Capabilities Development Command
DPR	downwelling path radiance
FOV	field of view
FTIR	Fourier transform infrared
H <sub>2</sub> O	purge water
InSb	Indium antimonide
LABB	large area blackbody
LWIR	long-wave infrared
MCT	mercury cadmium telluride
MODTRAN	MODerate resolution atmospheric TRANsmission
MWIR	mid-wave infrared
NIR	near-infrared
OPD	optical path difference
TN	technical note
UV	ultraviolet
VIS	visible
ZPD	zero-path difference

---

---

## **ORGANIZATION**

DEVCOM Analysis Center  
FCDD-DAE-E/B. Holtsberry  
White Sands Missile Range, NM 88002

DEVCOM Army Research Laboratory  
FCDD-RLD-DCI/Tech Library  
2800 Powder Mill Rd.  
Adelphi, MD 20783

Defense Technical Information Center  
ATTN: DTIC-O  
8725 John J. Kingman Rd.  
Fort Belvoir, VA 22060-6218